2011 IEEE/RSJ International Conference on
Intelligent Robots and Systems
September 25-30, 2011. San Francisco, CA, USA

Passive undulatory gaits enhance walking in a myriapod millirobot

Katie L. Hoffman and Robert J. Wood

Abstract— **The design and modeling of a segmented myriapod millirobot with a compliant body is presented. A dynamic model is used to demonstrate how body undulations can result from only varying the phase difference in the stance change between adjacent segments - even with passive intersegmental connections - and how these gaits affect locomotion. Different gaits are demonstrated experimentally in a 20-leg, 2.2 gram millirobot, and the resulting motion is compared to that predicted by the simulation. Both simulation and experiments show that undulatory gaits can increase the average speed of straight-line locomotion as compared to non-undulatory gaits for the same stepping frequency. The model and the millirobot can be used concurrently with biological studies to understand aspects of myriapod locomotion. This robot is also a useful tool to gain insight into how flexibility can be introduced into robots at this scale to enhance locomotion.**

I. INTRODUCTION

In recent years, biological inspiration has accelerated the development of aerial, ambulatory, and aquatic robots. At the insect scale, these include ambulatory robots such as DynaRoACH, a 24 gram autonomous hexapod [1], HAMR, a 2 gram hexapod capable of speeds up to 4 body lengths/second [2], and DASH, a robust and agile 10 cm long hexapod [3]. The design of these millirobots was inspired by cockroaches who are among the fastest creatures on the planet (normalized to body length) at up to 40 body lengths/second [4]. Due to the relatively low number of articulated components and a nominally rigid body, it is natural to use these insects as inspiration for ambulatory robots. However, the diversity of body morphologies found in nature leaves open questions about ambulation at small scales. For example, why do arthropods have different numbers of legs? Why do some creatures have flexible bodies while others have rigid bodies with flexible appendages? How do passive dynamics affect walking? This paper looks to explore some of these questions using a centipede-inspired robot.

Although their bodies are much more elongated, centipedes are also agile creatures with maximum speeds around 10 body lengths per second [5]. The flexibility inherent in myriapods allows them to morph to surfaces and smoothly transition between horizontal and vertical surfaces. This flexibility also has the potential to enhance locomotion through the use of body undulations and enable rapid turns. The segmented nature of a centipede body suggests a modular design, which can be adapted for use in different situations. A many-legged robot could also be robust to leg failures, still capable of locomotion even after the loss of multiple legs, as is the case with actual centipedes. Increased static stability could result from the added number of legs on the ground at any time, and the center of mass is likely to always remain within the support tripod since more legs are distributed along the length of the body. While additional legs may increase the total number of components of the robot, due to the use of repeating segments, the number of unique components would not increase. The concurrent development of batch fabrication techniques for millirobots could allow centipede robots at this scale to be easily fabricated.

The authors are with the School of Engineering and Applied Sciences and the Wyss Institute for Biologically Inspired Engineering, Harvard University, Cambridge, MA 02138 khoffman@fas.harvard.edu

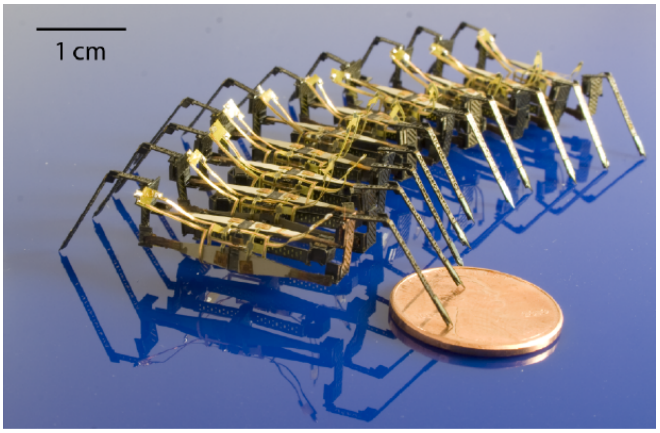

Fig. 1. Photo of a 10-segment, 20-leg centipede-inspired millirobot.

The effectiveness of undulatory gaits, or the wavelike motion of the body as depicted in Fig. 2(a), demonstrated by many centipedes have long been debated by biologists. Manton, who did visual studies on centipede locomotion and body morphology in the 1950's argued that the undulations were passive. At low speeds, these undulations were less pronounced as compared to when the same specimen were traveling at higher speeds [5]. This led her to the conclusion that at low speeds the centipedes were able to suppress any body waves that would naturally arise, whereas when moving faster, the centipedes were unable to actively work against the undulations. Conversely, while using both visual information as well as electromyograms attached to the lateral flexor muscles situated along the body of a centipede, Anderson found that centipedes actively promote body undulations [6]. Groups of legs form pivot points along the length of the body, which curves around the points (Fig. 2(a)). This body rotation may act to increase step size as compared to non-undulatory gaits (Fig. 2(b)).

Multiple robots have been modeled after centipedes, demonstrating the ability to create undulatory gaits, although at larger scales. Various gaits for a modular robot with

978-1-61284-455-8/11/$26.00 ©2011 IEEE

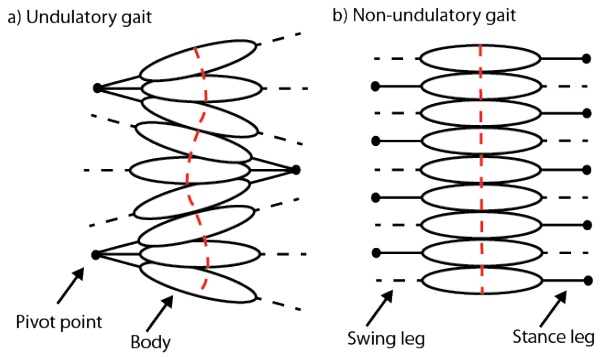

Fig. 2. Illustration of a) undulatory and b) non-undulatory gaits for a segmented creature, with red dashed line showing body curvature.

actuated rotational connections between segments were studied in simulation, with the conclusion that undulatory gaits could be faster than rigid-body gaits [7]. Various undulatory patterns, both with and without legs, were demonstrated in a five-segment robot also with active rotational joints between segments [8]. While centipede robots at larger scales exhibit the use of body undulations to achieve forward locomotion, many do not offer explanations of performance benefits from using undulatory gaits. These robots also all actively create undulations through actuated joints located between adjacent segments. This may require additional energy to control the amount of body rotation between adjacent segments.

The work presented here seeks to explore how undulations resulting from the use of passive mechanisms, located between segments of a 20-leg centipede millirobot, can enhance straight-line locomotion merely by changing the phase of the stance between adjacent segments. The notional design of this modular robot - a photo of the 20-leg version used in these experiments is shown in Fig. 1 - is presented along with the fabrication process used to create the device. A dynamic model of the horizontal plane motion is used to predict the locomotion of the millirobot and determine acceptable body and actuator parameters. Finally, undulatory and non-undulatory gaits of the robot are demonstrated both in simulation and experimentally and evaluated based on average speed and estimated cost of transport. This study shows that undulations resulting from passive intersegmental connections and only a change in phase of the stance of adjacent segments can increase step size and, therefore, average speed for similar work input.

II. NOTIONAL DESIGN AND FABRICATION

The millirobot design presented here has evolved from previous versions into a design similar in morphology to centipedes, which typically have repeating, two-legged segments, low-inertia legs, muscles at the proximal 'hip' joint to create leg motion, and a foot that pivots relative to the ground [5]. A rendering of the design of an individual segment is shown in Fig. 3. This design features centrally located actuators and lightweight legs to reduce the moment of inertia about the hip. Each segment has two orthogonal four-bar mechanisms, or transmissions, and two pairs of piezoelectric bimorph actuators [9], chosen for their high bandwidth, easy implementation, and the success of actuation by material deformation at this scale due to the deleterious scaling laws for other types of actuation. The four-bar mechanisms, which transform the linear actuator input into a rotational output, are composed of flexures rather than pure rotational joints to avoid losses due to friction. One bimorph pair, the 'stance' actuators, provides a linear input to a four bar mechanism which lift and lower each leg. Coupling of the drive signals allow one leg to be lifted while the other is placed on the ground. Similarly, the second bimorph pair, the 'swing' actuators, rotate the legs at the hip joint in the horizontal plane, providing a torque about the stance leg, while the swing leg is being reset in preparation for the next step. This design featuring coupled drive signals promotes simplicity by reducing the number of drive signals necessary for coordinated control of each leg to two.

The legs are attached to the output of the transmission and angled outward to facilitate lifting. The millirobot shown in Fig. 1 achieves a leg lifting height of approximately 3-4 mm, compared to the 1 cm body height. The swing distance is dependent on the gait being used and, as described in Sec. IV, increases for undulatory gaits due to interactions between adjacent segments. To allow the feet to rotate with respect to the horizontal plane but not slip laterally or in the direction of motion, pointed feet fabricated from 75 μm stainless steel are attached to the base of each leg. The sharp tip allows the feet to act as a pin joint with respect to ground, an assumption made in the dynamic model presented in Sec. III.

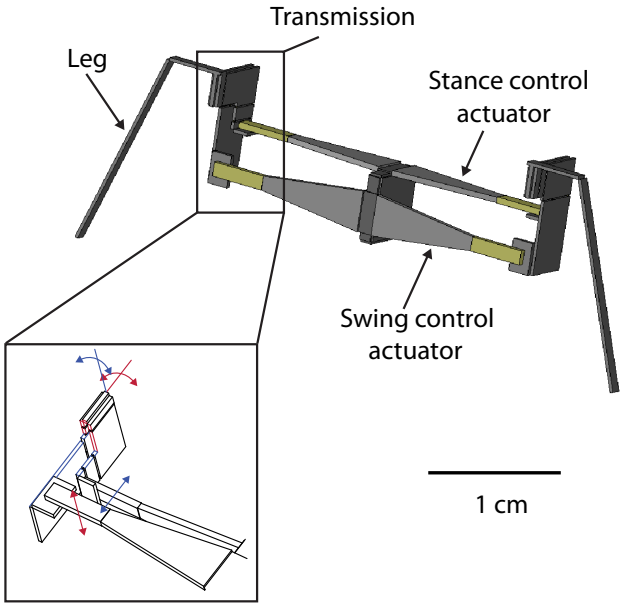

Fig. 3. Rendering of an individual segment with transmission detail showing the linear actuator inputs being transformed into rotational outputs.

Individual segments are integrated into a single structure through the use of a flexible backbone. The goal of the backbone is to provide each segment with the same number of degrees of freedom and enough degrees of freedom to

have an independent drive signal but still allow dynamic feedback between adjacent segments. A passive backbone was chosen to simplify the robot as well as study how body undulations naturally arise due to the dynamics of the system; however, active backbone joints could be integrated in future versions. An individual intersegmental connection as well as a rendering of a five-segment robot are shown in Fig. 4 and Fig. 5, respectively. Each connection has a linear joint (Sarrus linkage) sandwiched between two rotational joints (flexures) situated along the length of the body. This connection is mirrored on both sides of the body to allow the motion of adjacent segments to provide opposing moments about the center of mass and increase stability. Both linear and rotational joints were chosen to give each segment the freedom to rotate relative to adjacent segments and allow the entire body to extend and compress. The Sarrus linkage is fabricated in a pre-compressed state to allow both extension and compression. An actual backbone is shown in Fig. 4(b-d) undeformed, compressed, and rotated, respectively. The backbone was designed to allow relative motion between each segment in the horizontal plane but be resistant to off-axis rotations. The modular design of the robot allows any number of segments and backbone structures to be attached to enable comparisons across robots with increasing number of legs. For the millirobot used in the experiments described here (Fig. 1), each segment with attached backbone structure measures 1 cm by 1 cm by 4 cm wide.

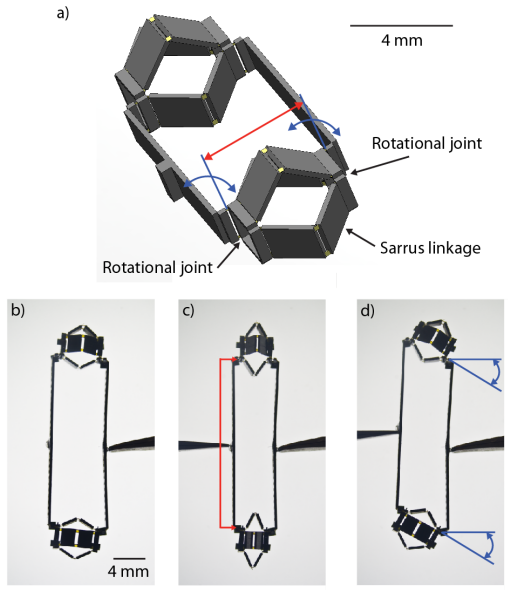

Fig. 4. a) Rendering of an intersegmental connection illustrating passive linear and rotational joints and a top view of an actual backbone b) undeformed, c) compressed, and d) rotated.

The millirobot is fabricated using a modified version of the Smart Composite Microstructures (SCM) process presented in [10],[11]. The flexure joints are created with a thin film (polyimide), and the rigid links are made from Carbon Fiber. The millirobot currently does not have on-board electronics and is controlled and powered by an

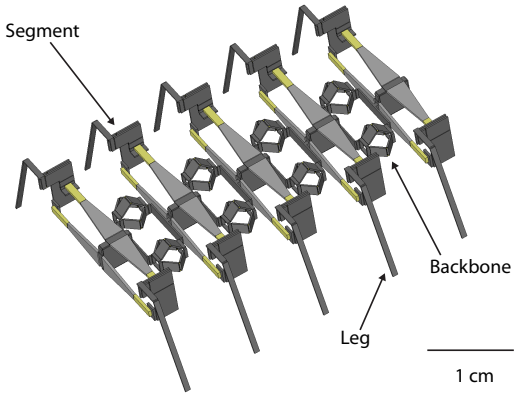

Fig. 5. Five segment robot illustration, demonstrating the connection between segments and backbone components.

external xPC target system (Mathworks) and high voltage amplifier. The experiments described in Sec. IV use square waves alternating between 0 and 200 V, albeit current on the order of mA, for stance and swing control. To minimize wiring, flexible circuits are created from copper-clad Kapton using a modified lithography process, where exposure is performed by direct write using an ultraviolet (UV) laser. The circuits connect each ground and high voltage signal per segment, eliminating the need to individually wire each actuator; however, two wires per segment are still necessary to deliver power from an external supply. Wires 50 μm in diameter are used to reduce interference with locomotion. Future work will focus on onboard electronics similar to those presented in [12].

III. MODELING

To determine how to excite undulatory modes using a passive, flexible body and quantify the effect of undulatory gaits, a dynamic model was created to describe the motion of the robot. Since the undulations occur in the horizontal plane of the robot on flat terrain, the model is limited to this plane. There is assumed to be no coupling between the horizontal and vertical plane motion, and, therefore, the stance is determined by a binary input. Due to the modular nature of the robot, the dynamics can also be written in a modular fashion, facilitating studies involving robots with any number of legs. A physical description of the model is shown in Fig. 6. A torque τ_i is applied about the hip joint of each segment. The leg is free to rotate relative to ground by an angle α_i, and the body can rotate an angle θ_i, both with respect to an axis perpendicular to the direction of motion. The state variables for each segment are the leg and body rotations as well as the leg and body angular velocities, $\dot{\alpha}_i$ and $\dot{\theta}_i$. Having only one control input in the horizontal plane, but two degrees of freedom per segment makes this robot underactuated. Important geometries include the leg length L_{leg}, the body width w_b measured between hip joints, the body length L_b in the direction of motion, and the equilibrium length of the Sarrus linkage l_s. The kinematics of each segment, or the position of every point on the robot,

can be written in terms of α_i, θ_i, and the current position of the stance foot.

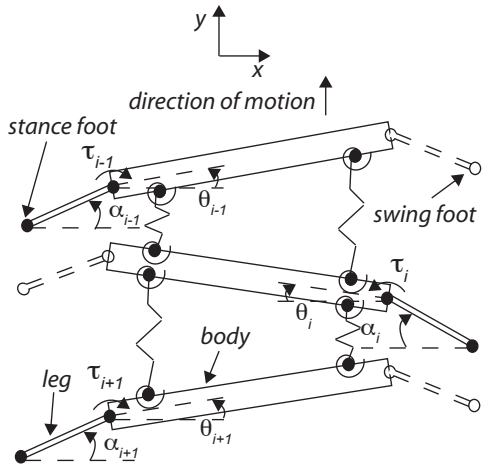

Fig. 6. Depiction of horizontal plane motion of a three segment millirobot.

The mass m of each segment is concentrated in the body as the actuators constitute the majority of the mass, and the legs are assumed to be massless and rigid. The total kinetic energy can then be calculated according to

$$K = \frac{1}{2}\sum_{i=1}^{n} I_{cm}\dot{\theta_i}^2 + m(\dot{x_i}^2 + \dot{y_i}^2) \tag{1}$$

where I_{cm} is the moment of inertia about the center of mass. $\dot{x_i}$ and $\dot{y_i}$ are the velocities of the center of mass, which can be written in terms of the state variables using the kinematics of the system. This is not shown here for brevity. The total kinetic energy is summed over all n segments.

The potential energy for the system includes that stored in the flexures and Sarrus linkages forming the intersegmental connections as well as that of the piezoelectric actuator, which is modeled as a force source in parallel with a spring and damper [13]. This is calculated as follows:

$$P = \frac{1}{2}\sum_{i=1}^{n-1} k_l(\Delta l_{ac,i}{}^2 + \Delta l_{bd,i}{}^2) + k_t(\gamma_{a,i}^2 + \gamma_{b,i}^2 + \gamma_{c,i}^2 + \gamma_{d,i}^2) + \frac{1}{2}\sum_{i=1}^{n} k_a \frac{1}{T_h^2}(\alpha_i - \theta_i)^2 \tag{2}$$

where k_l is the linear spring constant for the Sarrus linkage, k_t is the torsional spring constant of the backbone rotational joints, $\Delta l_{ac,i}$ and $\Delta l_{bd,i}$ are the Sarrus linkage deflections, and $\gamma_{a,i}$, $\gamma_{b,i}$, $\gamma_{c,i}$, and $\gamma_{d,i}$ are the rotations of the backbone torsional springs. The deflections and rotations for each portion of the backbone can be written out in terms of the state variables of each adjacent segment using the kinematics of the robot. The stiffness of the rotational springs can be found using basic bending beam theory, and the stiffness and range of deflection of the Sarrus linkage is found using a finite element model. k_a is the actuator stiffness, which is mapped through the four-bar transmission with transmission ratio T_h. The potential energy stored in the flexures of the four-bar mechanism is assumed to be negligible.

TABLE I
CENTIPEDE MILLIROBOT PARAMETERS

Leg length, L_{leg}	10 mm
Body length, L_b	3 mm
Body width, w_b	20 mm
Sarrus linkage length, l_s	4 mm
Transmission ratio, T_h	2.5 rad/mm
Actuator stiffness, k_a	860 N/m
Sarrus linkage stiffness, k_l	29 N/m
Backbone flexure stiffness, k_t	7.6 $\mu Nm/rad$
Maximum torque, $\tau_{i,max}$	34.5 μNm
Actuator damping, b_a	6.3 Ns/m
Segment mass, m	220 mg
Segment inertia, I_{cm}	8.1×10^{-3} mgm^2

Finally, the work transfer can be characterized by the torque input from the actuators, τ_i (mapped through the four-bar mechanism) and the losses due to actuator damping as described by

$$W = \sum_{i=1}^{n} \tau_i(\alpha_i - \theta_i) - b_a \frac{1}{T_h^2}(\alpha_i - \theta_i)(\dot{\alpha_i} - \dot{\theta_i}) \tag{3}$$

where b_a is the actuator damping constant, calculated using material properties [13]. The losses from the transmission and other flexures is assumed to be negligible as measured for a similar mechanism [14]. The friction on the foot, which is assumed to be a pin joint, is also not included in this model. The feet are designed to come to a sharp point to facilitate rotation and reduce sliding friction. A more detailed study of the losses in the system would yield better predictions of overall performance; however, this is outside the scope of this work, which is looking for trends arising from undulations due to segment phase.

The Euler-Lagrange method and these energy terms were used to formulate the equations of motion for an n-segment millirobot. A simulation was created describing the motion of the robot. The complexity of the coupled, nonlinear equations required the use of a numerical differential equation solver. The hybrid dynamic nature of the robot allows for the use of the derived equations over one step; however, collisions occurring when the stance changes requires calculating new initial conditions for the state variables. It is assumed that these collisions are inelastic and instantaneous. This is done using conservation of momentum about the stance foot and hip joint when changing stance [15].

The dynamic simulation was used to determine parameters for the millirobot shown in Fig. 1 with relevant parameters listed in Tab. I. The geometries and actuator parameters were chosen to avoid collisions between adjacent legs over the range of gaits studied. The spring constants for the backbone were determined to provide sufficient feedback between segments, while being compliant enough to allow undulations to arise. A more thorough discussion of the effects of these parameters on locomotion is given in Sec. IV.

IV. LOCOMOTION STUDIES

To study how body undulations affect locomotion of many-legged creatures and how these undulations can arise passively, simulations and experiments of the robot for

various frequencies and phase differences were performed. Using the experimental system parameters, varying the phase between adjacent segments, holding the leg cycle frequency constant at 5 Hz, and applying a constant torque about each stance leg, the motion of the system was simulated for 500 steps for each phase between 40 and 180 degrees. The drive signal for each individual segment was held constant at a specified torque for each gait; only the timing of stance change between adjacent segments was altered. This was done for a 10-segment, 20-leg robot, due to the wide variety of gaits that can be performed with this number of legs. At a phase difference of 180 degrees, all adjacent segments have opposite stance feet, similar to the alternating tripod gait used by hexapods. Below a phase difference of 40 degrees, or $360/(n-1)$ degrees where n is the number of segments, a 10-segment robot is not statically stable in the vertical plane, as clumps of legs no longer form a tripod. The results of the simulated motion are shown in Fig. 7.

Only stable solutions were plotted, with stability in the horizontal plane being defined as no collisions between adjacent segments (for 500 steps). The lack of data points between a phase of 97 and 172 degrees in Fig. 7 indicates a region of unstable gaits. In this region, there are only clumps of one and two legs. With many groups of legs distributed along the length of the body, legs are switching groups too quickly to pull the following segment along the same path as the previous segment, failing to reach a limit cycle and eventually resulting in collisions between segments. At smaller phases and, therefore, larger groups of three or four legs, a single segment constitutes a smaller portion of the whole group, thus being easily pulled along the same path as previous segments when switching between groups of legs as stance changes. Additionally, this does not happen for phases around 180 degrees due to symmetry that comes with adjacent segments having opposite stance feet.

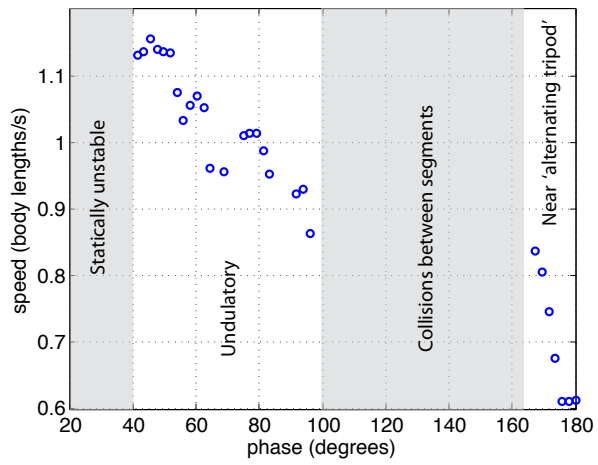

Fig. 7. Simulated average speed at 5 Hz stepping frequency as a function of phase difference between adjacent segments. Only stable solutions are plotted.

The interesting part of this study is that the average speed decreases from a maximum at a phase difference of 45 degrees to a minimum at 180 degrees, or the same phase used in the alternating tripod gait in hexapods. The reason for the difference in average speed can be deciphered by looking at the amount of body rotation θ and leg rotation α for each segment when the stance changes. For a phase difference of 180 degrees, when alternating segments have opposite stance feet, the body of the segments rotate backwards as the leg is rotating forward. Due to the opposite rotation of adjacent segments, the body will be pulled forward to an equilibrium rotation of zero degrees, causing no amplification in step size. For this gait, the leg rotates forward significantly, but springs back slightly, oscillating around a positive equilibrium position. The forward rotation of the leg is larger than the backwards rotation of the body, resulting in a net forward motion of the robot. Conversely, for phase differences between 45 and 60 degrees, clumps of legs form pivot points around which the body and legs rotate. The body rotates forward until the segment switches feet when at a positive body rotation. To minimize the energy stored in the backbone springs, the body curves around the pivot points for a group of legs, causing this positive body rotation, increased rotation of stance legs, and wave-like motion of the center of mass of each segment, resulting in amplification of step size. Here, undulations almost double step size compared to the non-undulatory gait (phase of 180 degrees).

Not only is the average speed for phases between 45 and 60 degrees (undulatory gaits) the largest for these operating conditions, but the body undulations demonstrated by these gaits are qualitatively similar to those of real centipedes [6],[5]. As can be seen for a phase of 60 degrees in the frames of motion in Fig. 8, the legs form clumps pointing in towards a pivot point, while the centers of mass of the segments form a traveling wave along the length of the body. This shows that even though the design is underactuated, body undulations mimicking those of actual centipedes are expected to result from the natural system dynamics, causing increases in speed for the same leg cycle frequency and body parameters as compared to non-undulatory gaits.

To explore gaits over a range of frequencies, two representative gaits were chosen. The first gait is characterized by a phase of 180 degrees between adjacent segments, termed the 'non-undulatory gait.' The second gait uses a phase of 60 degrees, an 'undulatory gait'. While a phase of 45 degrees should result in a faster average speed, a phase of 60 degrees allows drive signals to be shared between segments, which is beneficial for the experimental system. As shown in Fig. 9(a), the undulatory gait was found to produce a higher average speed than the 'non-undulatory' gait for a range of frequencies. For a phase of 60 degrees, the motion over the range of frequencies was found to be similar to that described above and shown in Fig. 8. The degree of body and leg rotation, or the magnitude of the resulting undulations, varied slightly across frequencies. For a phase of 180 degrees, at low frequencies, the body and legs would rotate backwards and forwards respectively, but spring back to a smaller equilibrium value due to adjacent segments rotating in the opposite direction. This occurred

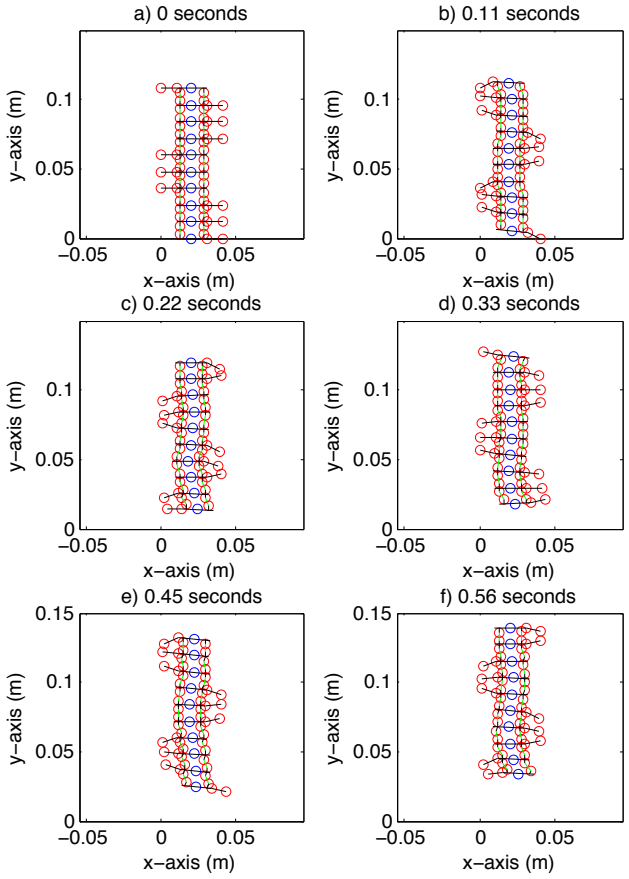

Fig. 8. Simulated undulatory motion using a 60 degree phase difference between adjacent segments at a 3 Hz leg frequency. The red circles indicate the stance feet and hip joints, the blue circles represent the center of mass of each segment, the green lines are the Sarrus linkages, and the black lines are the body and legs. The swing legs are not shown. For videos demonstrating the simulated motion, see the Supplementary Material.

mainly for frequencies up to 8 Hz; however, beyond 8 Hz, it is possible to see that the gap in average speed between a phase of 60 and 180 degrees begins to close. The decreased difference in speed is due to stance changing before the legs can fully spring back to the equilibrium position for a phase of 180 degrees. While driving the robot at a frequency that will cause the stance to change when the leg has rotated forward the most, which for the parameters chosen here is approximately 12 Hz, an undulatory gait at the same frequency is still predicted in simulation to perform better. This is due to the initial backwards rotation of the body for a phase of 180 degrees during each step while for the undulatory gaits, the body is always rotating in the direction of locomotion. The segment natural frequency of 12 Hz is dictated by the segment inertia and actuator spring and damping constants. Simulations of both gaits are included in the supplemental video.

To verify the simulation predictions, a selection of gaits and leg cycle frequencies were tested in the 20-legged experimental device on flat cardstock. The average speeds were recorded for each frequency and are shown in Fig. 9(b). For all frequencies except for 10 Hz, a phase of 60 degrees was as fast as or faster than that of 180 degrees. Similar motion was observed experimentally as was predicted in simulation, demonstrating that passive undulations can arise merely by altering the phase of the stance change between segments (see supplemental video). Frames of motion for a video of this gait at a frequency of 3 Hz are shown in Fig. 10. Alternatively, as in simulation, for a phase of 180 degrees, the legs rotate forward, but spring back to an equilibrium position by the time the stance changed, while the body of each segment rotates backward but springs forward to an equilibrium rotation of zero degrees. The leg and body rotation at the time of stance change, which affects the step size, was confirmed for each gait at 1 and 3 Hz using videos and motion analysis software (ProAnalyst). The experimental and simulated body and leg angles are recorded in Tab. II. As can be seen, the average angles at the time of switching are larger for a phase of 60 degrees. The maximum frequency tested here was 10 Hz, at which the robot reached a speed of approximately 7 cm/second. The actuators can be driven at higher frequencies, although the robot performance at higher frequencies was not tested at this time. Videos for the undulatory and non-undulatory gaits are provided with the Supplementary Material.

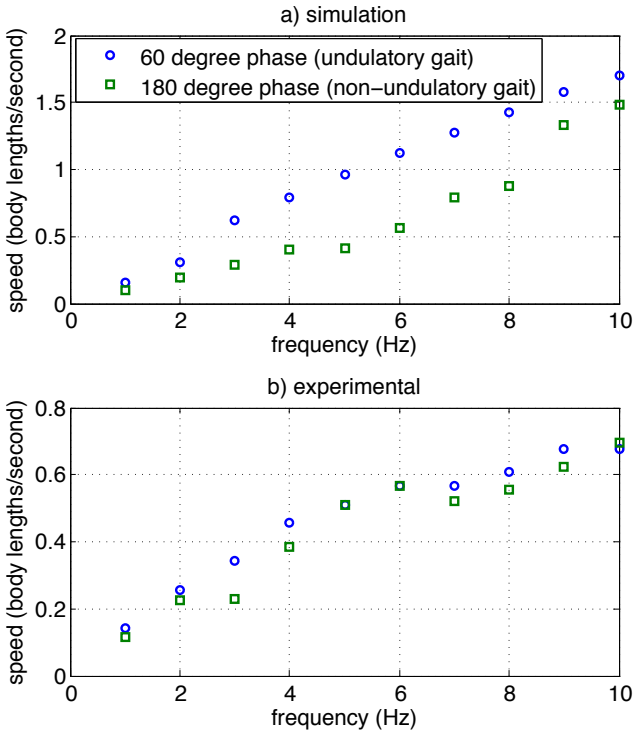

Fig. 9. a) Simulated and b) experimental average speeds for phase differences of 60 degrees and 180 degrees over a range of frequencies.

For both phases, the center of mass (COM) of the middle segment was tracked experimentally and predicted in simulation for frequencies of 1 and 3 Hz. The COM position in the direction of motion of the millirobot was plotted as a function of time. These are shown in Fig. 11. As can be seen both in simulation and experiment, for a phase of 180 degrees, the COM moves forward, but springs back and

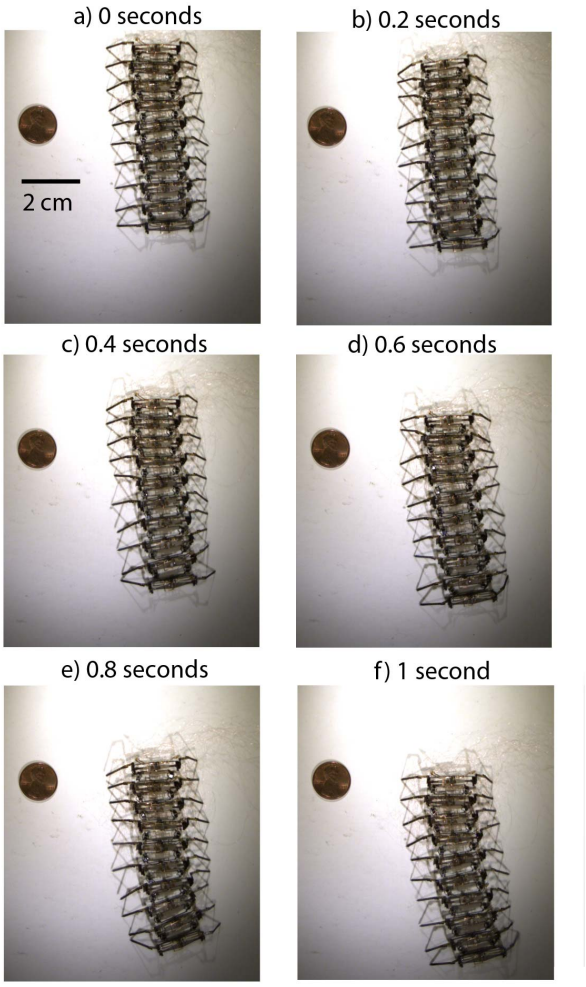

Fig. 10. Frames of motion from experiments using a 60 degree phase difference of the stance of adjacent segments at a 3 Hz leg frequency. Videos of the motion for different frequencies and phases are presented in the Supplementary Material.

TABLE II

AVERAGE BODY ROTATION θ AND AND LEG ANGLE α (DEGREES) AT STANCE CHANGE AVERAGED OVER 10 SEGMENTS FOR 5 STEPS

F (Hz)	Phase (deg)	α_{sim}	θ_{sim}	α_{exp}	θ_{exp}
1	60	40.9	2.7	30	2.2
	180	26.6	0	25	-0.2
3	60	50.3	4.4	20	0.9
	180	26.5	0	15	0.2

oscillates around an equilibrium position. When the COM moves opposite of the desired locomotion direction, energy is wasted. Alternatively, for a phase of 60 degrees both the simulation and experiments show the COM spring back slightly for a frequency of 1 Hz, but move steadily forward for a frequency of 3 Hz. The undulations that arise for this gait allow for a smooth forward motion of the center of mass.

The simulation was used to calculate the absolute value of the mechanical work per unit distance traveled per mass, or cost of transport, for each gait. Fig. 12 shows that the undulatory gait requires less work per unit distance as a result of negative body rotation for a portion of each step for the non-undulatory gait. Efficient locomotion is particularly important for small-scale robots, which generally have limited power supplies.

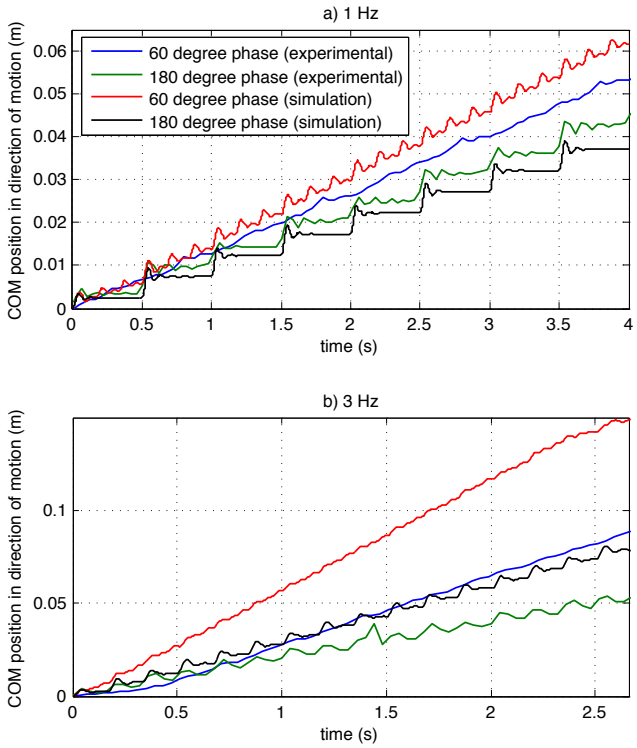

Fig. 11. Experimental and simulated center of mass position for 60 and 180 degree phases at a) 1 Hz and b) 3 Hz.

While the trends for locomotion are similar for the simulation and experiments, the experimental average speed is generally smaller than that predicted in simulation, and the body undulations are not as pronounced. Unmodeled foot slipping, flexure damping, or coupling between horizontal and vertical plane motion could contribute to the slower experimental speeds. Motion could also be affected by fabrication differences between segments due to manual assembly steps. Any differences in performance of a segment affects the motion of adjacent segments. External wiring may have an effect on locomotion as well.

This study was performed with specific body parameters, although the geometries and compliances affect the severity of undulations. For example, for a stiffer backbone, body undulations will be less pronounced; however, similar trends as shown here still occur. Increasing the stiffness of the backbone as much as two orders of magnitude still results in enhanced locomotion with undulatory gaits as compared to a non-undulatory gait, or phase of 180 degrees. This is due to the initial negative body rotation for a phase of 180 degrees as opposed to the positive body rotation for the undulatory gaits, although less pronounced than those with a more compliant backbone. Conversely, for a more compliant backbone, there will be less feedback between segments, leading to collisions between segments. The effect of parameters on undulatory gaits is the focus of future work.

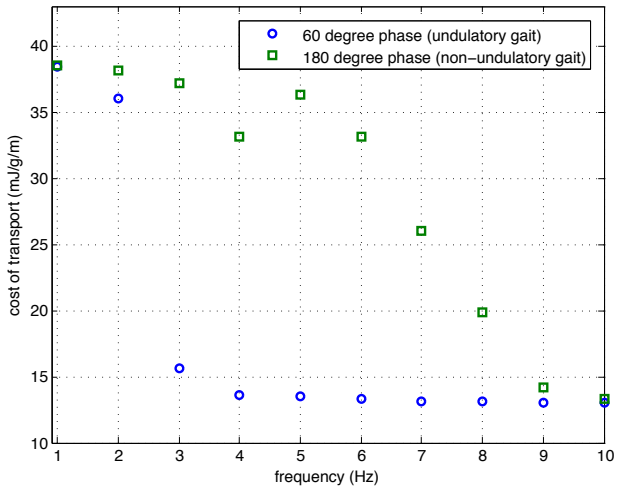

Fig. 12. Cost of transport for phases of 60 degrees and 180 degrees from simulation.

V. CONCLUSIONS AND FUTURE WORK

The work presented here demonstrates locomotion enhancement using undulatory gaits in a centipede millirobot. Increased leg and body angles for an undulatory gait, which arise due to the passive dynamics of the system, were shown to increase the average speed of the millirobot compared to a non-undulatory gait. This suggests millirobots inspired by the body morphology of centipedes can see improved straight-line locomotion by using undulatory gaits that feature groups of legs pointing towards similar pivot points distributed along the length of the body. Similar gaits have been found in nature [6], [5].

While the results shown here demonstrate that undulatory gaits in a centipede-inspired millirobot can enhance straight-line locomotion, the effect of physical parameters, such as geometry, stiffnesses, actuator characteristics and number of legs, were not studied extensively. Future work will focus on examining the effect of parameters on undulatory patterns and locomotion performance.

This millirobot offers the potential to study many different characteristics of legged robots at this scale. The modular design will enable a comparison between robots with different numbers of legs. Studies will determine if there is an optimal number of legs for a centipede-inspired millirobot in terms of robustness, speed, efficiency, and stability.

Passive body flexibility in the horizontal plane was used to create undulations during straight-line locomotion, but future work will focus on using this flexibility to perform dynamic turns. Additionally, a benefit of body flexibility in actual centipedes is the ability to morph to surfaces and easily transition between horizontal and vertical surfaces. Degrees of freedom will be added to the backbone to allow body flexibility in the vertical plane.

Robotic platforms such as the one presented here may be used to answer questions pertaining to how differing body morphologies affect walking at small scales. Using these systems, it is possible to understand how the passive dynamics resulting from different body types, whether myriapods or hexapods with flexible or rigid bodies, alter the effectiveness of different gaits. The insights gained can improve the design of walking robots at this scale.

VI. ACKNOWLEDGMENTS

This work was partially supported by the Wyss Institute for Biologically Inspired Engineering (Harvard University) and the National Science Foundation (under award number IIS-0811571). Any opinions, findings and conclusions or recommendations expressed in this material are those of the authors and do not necessarily reflect those of the National Science Foundation. This research was also made with Government support under and awarded by DoD, Air Force Office of Scientific Research, National Defense Science and Engineering Graduate (NDSEG) Fellowship, 32 CFR 168a.

REFERENCES

[1] A. Hoover, S. Burden, X. Fu, S. Sastry, and R. Fearing, "Bio-inspired design and dynamic maneuverability of a minimally actuated six-legged robot," in *IEEE International Conference on Biomedical Robotics and Biomechatronics*, 2010.

[2] A. Baisch, P. Sreetharan, and R. Wood, "Biologically inspired locomotion of an insect scale hexapod robot," *Proc. IEEE/RSJ International Conference on Intelligent Robots and Systems*, 2010.

[3] P. Birkmeyer, K. Peterson, and R. Fearing, "DASH: A Dynamic 16g Hexapedal Robot," *Proc. IEEE/RSJ International Conference on Intelligent Robots and Systems*, 2009.

[4] R. Full and M. Tu, "Mechanics of a rapid running insect: two-, four- and six-legged locomotion," *Journal of Experimental Biology*, vol. 156, pp. 215–231, 1991.

[5] S. Manton and M. Harding, "The evolution of Arthropodan locomotory mechanisms - Part 3. The locomotion of the Chilopoda and Pauropoda," *Journal of the Linnean Society of London, Zoology*, vol. 42, no. 284, pp. 118–167, 1952.

[6] B. Anderson, J. Shultz, and B. Jayne, "Axial kinematics and muscle activity during terrestrial locomotion of the centipede Scolopendra heros," *Journal of Experimental Biology*, vol. 198, no. 5, pp. 1185–1195, 1995.

[7] B. Jimenez and A. Ikspeert, "Centipede robot locomotion," Master's thesis, Ecole Polytechnique Federale de Lausanne, 2007.

[8] M. Sfakiotakis and D. Tsakiris, "Undulatory and pedundulatory robotic locomotion via direct and retrograde body waves," *IEEE International Conference on Robotics and Automation*, pp. 3457–3463, 2009.

[9] R. Wood, E. Steltz, and R. Fearing, "Optimal energy density piezoelectric bending actuators," *Sensors & Actuators: A. Physical*, vol. 119, no. 2, pp. 476–488, 2005.

[10] R. Wood, S. Avadhanula, R. Sahai, E. Steltz, and R. Fearing, "Microrobot design using fiber reinforced composites," *Journal of Mechanical Design*, vol. 130, no. 5, p. 052304, 2008.

[11] K. Hoffman and R. Wood, "Towards a multi-segment ambulatory microrobot," *Proc. IEEE International Conference on Robotics and Automation*, 2010.

[12] M. Karpelson, G.-Y. Wei, and R. Wood, "Milligram-scale high-voltage power electronics for piezoelectric microrobots," *IEEE International Conference on Robotics and Automation*, 2009.

[13] R. Wood, E. Steltz, and R. Fearing, "Nonlinear performance limits for high energy density piezoelectric bending actuators," *IEEE International Conference on Robotics and Automation*, pp. 3633–3640, 2005.

[14] E. Steltz, M. Seeman, S. Avadhanula, and R. Fearing, "Power electronics design choice for piezoelectric microrobots," in *IEEE/RSJ International Conference on Intelligent Robots and Systems*, 2006, pp. 1322–1328.

[15] V. Chen and R. Tedrake, "Passive dynamic walking with knees: a point foot model," Ph.D. dissertation, Massachusetts Institute of Technology, 2007.